Disorder effects near a magnetic instability in $CePtSi_{1-x}Ge_x$ ($x=0$, 0.1)

Ben-Li Young,[1,2,*] D. E. MacLaughlin,[1] M. S. Rose,[1] K. Ishida,[1,3,†] O. O. Bernal,[4] H. G. Lukefahr,[5] K. Heuser,[6] G. R. Stewart,[7] N. P. Butch,[8] P.-C. Ho,[8] and M. B. Maple[8]

[1]*Department of Physics, University of California, Riverside, California 92521-0413, USA*

[2]*Condensed Matter and Thermal Physics, Los Alamos National Laboratory, Los Alamos, New Mexico 87545, USA*

[3]*Department of Physical Science, Graduate School of Engineering Science, Osaka University, Osaka 560-8531, Japan*

[4]*Department of Physics and Astronomy, California State University, Los Angeles, California 90032-8206, USA*

[5]*Whittier College, Whittier, California 90608, USA*

[6]*Institut für Physik, Universität Augsburg, D-86135 Augsburg, Germany*

[7]*Department of Physics, University of Florida, Gainesville, Florida 32611, USA*

[8]*Department of Physics and Institute for Pure and Applied Physical Sciences, University of California, San Diego, La Jolla, California 92093-0319, USA*

(Received 19 October 2002; revised manuscript received 19 March 2004; published 1 July 2004)

The magnetic susceptibility and nuclear magnetic resonance (NMR) linewidth have been measured in the heavy-fermion alloys $CePtSi_{1-x}Ge_x$, $x=0$ and 0.1, to study the role of disorder in the non-Fermi-liquid (NFL) behavior of this system. The theoretical NMR line shape is calculated from disorder-driven NFL models and shows the same essential features as the observed spectra. Analysis of ^{29}Si and ^{195}Pt NMR linewidths strongly suggests the existence of locally inhomogeneous susceptibility in both materials, and agrees with the widths of the local susceptibility distributions estimated from the susceptibility fits to the disorder-driven NFL models. Disorder-driven mechanisms can also explain the NFL behavior in $CePtSi_{0.9}Ge_{0.1}$; the NMR spectra do not, however, distinguish between the Kondo-disorder and Griffiths phase models. We find that stoichiometric CePtSi and Ge-doped $CePtSi_{0.9}Ge_{0.1}$ show similar degrees of magnetic disorder, although a narrower distribution of local susceptibilities in CePtSi allows Fermi-liquid behavior to appear below 1 K. The residual resistivity reported in CePtSi is relatively large, which indicates a significant level of intrinsic lattice defects and seems to be consistent with the disorder observed in the NMR spectra.

DOI: 10.1103/PhysRevB.70.024401 PACS number(s): 71.10.Hf

I. INTRODUCTION

The extraordinary behavior of magnetic, thermodynamic and transport properties (e.g., magnetic susceptibility $\chi \sim -\ln T$, specific heat coefficient $C/T \sim -\ln T$, and electrical resistivity $\rho \sim T$) found at very low temperatures in many Ce- and U-based heavy-fermion intermetallic alloys and compounds has been considered evidence for the breakdown of Landau Fermi-liquid (FL) theory,[1] and has been classified as non-Fermi-liquid (NFL) (Refs. 2 and 3) or singular Fermi-liquid[4] physics. Several mechanisms, such as unconventional Kondo effects,[5,6] proximity to a quantum critical point (QCP) in the phase diagram,[7–9] and structural disorder effects,[10–13] etc., have been proposed to explain the NFL phenomena.

A large number of the heavy-fermion systems which show NFL behavior at very low temperatures are found to be located near a QCP for an antiferromagnetic instability, at which the Néel temperature is suppressed to zero via doping,[14] or application of pressure[15] or magnetic field.[16] The balance between the Kondo effect and the Ruderman-Kittel-Kasuya-Yosida (RKKY) interaction seems to play a crucial role. However, some NFL systems are found far from a QCP, e.g., $U_xY_{1-x}Pd_3$ (Ref. 17) and $UCu_{5-x}Pd_x$,[18] where the QCP scenario may not be favorable. On the other hand, the chemical compositions of many NFL materials are not in a stoichiometric form (either *f* ions or non-*f* ligand atoms are substituted with other atoms), and thus intrinsic structural disorder has also been suspected to play an important role as well. Nevertheless, structurally ordered NFL systems also exist. For example, $CeNi_2Ge_2$,[19] $YbRb_2Si_2$,[20] and UBe_{13} (Ref. 21) are among the known stoichiometric NFL systems where the disorder-driven NFL picture may not be applicable.

Structural order is often found in a stoichiometric compound, but it is not guaranteed. The heavy-fermion compound $CeAl_3$ has been reported to have a spatial magnetic inhomogeneity,[22] which implies a certain amount of disorder. In addition, sample preparation (e.g., annealing) is an important issue in several NFL systems. Local defects, strains, or second phases can alter the low-temperature properties significantly, and thus make a disorder-driven NFL picture possible.

To date, the Kondo-disorder[10,11] and Griffiths phase models[12,13] are the primary disorder-based NFL theories. The compounds $UCu_{3.5}Pd_{1.5}$ (Ref. 23) and $Y_{0.8}U_{0.2}Pd_3$ (Ref. 24) (far from a QCP) and $CeRhRuSi_2$ (Ref. 25) (near a QCP) have been found to agree with the disorder-driven NFL models. However, disorder effects in the stoichiometric compound UCu_4Pd are still questionable. Booth *et al.*[26] claim that the microscopic lattice disorder (Pd/Cu site interchange) observed in the x-ray-absorption fine-structure (XAFS) experiment is a possible source for the NFL behavior in this material. Recently Weber *et al.*[27] have used annealing as a control parameter and observed that the NFL properties are strongly modified in annealed UCu_4Pd, which they argue

contradicts the disorder-induced NFL picture. Nevertheless the annealing experiment still emphasizes the influence of lattice disorder on the electronic ground states.

Quantum criticality has been studied in $CeCu_{6-x}Au_x$,[28] where NFL behavior appears at a critical concentration of $x=0.1$. The behavior of this system can be modified by applying a magnetic field or pressure. It is believed that unusual spin fluctuations at zero temperature quantum phase transition dominate the NFL behavior. Narrow muon-spin relaxation (μSR) spectra[23] and the low residual resistivity are evidence against the importance of disorder effects in $CeCu_{5.9}Au_{0.1}$.

$CePtSi_{1-x}Ge_x$ (Ref. 29) has a very similar phase diagram to that of $CeCu_{6-x}Au_x$.[28] CePtSi is a typical heavy-fermion system, and shows FL behavior in the specific heat below 1 K.[30] Upon doping with Ge, the FL behavior is suppressed, and $CePtSi_{1-x}Ge_x$ reaches a QCP at a concentration of $x=0.1$. Further Ge doping increases the Néel temperature T_N, and the system enters an antiferromagnetic ground state. Since the disorder-driven NFL models have successfully described NFL systems which are far from a QCP, we have performed NMR experiments in the heavy-fermion alloys $CePtSi_{1-x}Ge_x$, $x=0$ and 0.1, in order to further check the role of disorder effects in a system near a magnetic instability. This system gives us an opportunity to study how structural disorder is involved in changing the low temperature properties from an ordered Fermi liquid ($x=0$) to a ligand-disordered non-Fermi-liquid system ($x=0.1$).

$CePtSi_{1-x}Ge_x$ is a good system for a NMR study. The ^{29}Si nucleus has been used as the primary probe nucleus in the present work, and ^{195}Pt NMR has also provided an independent probe to check the results. ^{29}Si and ^{195}Pt are both spin-1/2 nuclei so that quadrupolar effects are absent, and all ^{29}Si (^{195}Pt) sites in the tetragonal unit cell are equivalent (see Fig. 1). Thanks to these two advantages, NMR frequency shifts and line shapes in $CePtSi_{1-x}Ge_x$ can be analyzed easily and accurately. Thus the full theoretical NMR spectra based on the disorder-driven NFL models can be compared with the observed spectra.

Our NMR results reveal that, surprisingly, the degree of magnetic disorder in the stoichiometric compound CePtSi is similar to that in the 10% Ge-doped sample. This is, however, consistent with the relatively high residual resistivity reported in CePtSi, which suggests the existence of intrinsic lattice disorder. Correlation between disorder in spin dynamics and the residual resistivity has been reported in Ref. 31.

In many Ce-based heavy-fermion compounds, the bulk susceptibility can be described well in terms of the single-ion Ce^{3+} susceptibility. By convoluting the single-ion susceptibility with the susceptibility distribution given by disorder-driven NFL models, the bulk (average) susceptibility can be calculated. If there is disorder-induced magnetic inhomogeneity, this distribution can be determined by fitting the experimental susceptibility data to the calculated bulk susceptibility. Then the estimated susceptibility distribution can be used to examine the NMR linewidth quantitatively in order to understand if the observed NMR line broadening is caused by the inhomogeneous susceptibility. Due to the strong tetragonal crystalline electric field (CEF) effect in $CePtSi_{1-x}Ge_x$,[32] the single-ion susceptibility used in this procedure has been calculated including the CEF splitting of the Ce^{3+} ion.

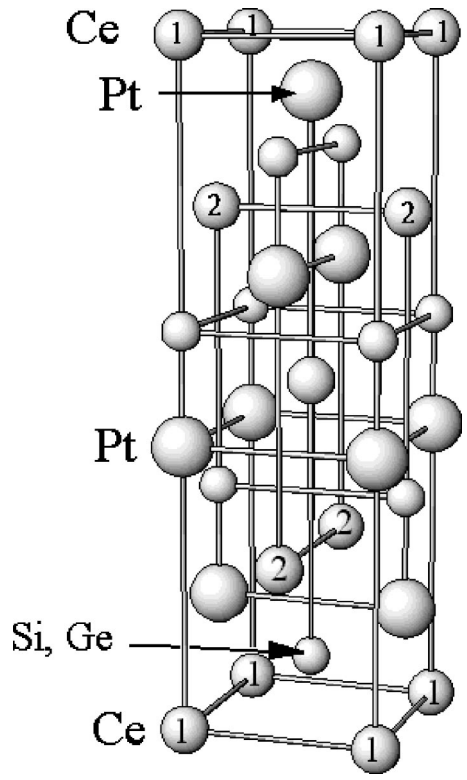

FIG. 1. Tetragonal crystal structure of $CePtSi_{1-x}Ge_x$. Each Si or Pt site has four nearest Ce neighbors (No. 1) and two Ce next-nearest neighbors (No. 2).

The temperature dependence of the magnetic susceptibility measured from room temperature down to 2 K in both CePtSi and $CePtSi_{0.9}Ge_{0.1}$ was originally used to perform the susceptibility fits. However, we found that the lack of low temperature data substantially affected the fit results for CePtSi, because only below 1 K is there evidence from measurements of the specific heat $C(T)$ that CePtSi returns to the FL state.[30,33] Unfortunately, our magnetization measurements below 1 K show that the possible spurious magnetic phase strongly affects the low temperature susceptibility such that the expected signature of FL-like susceptibility in CePtSi is suppressed (see Sec. II D). In order to bypass this problem, we therefore have estimated the susceptibility $\chi(T)$ down to 0.1 K from the specific heat data and the extrapolated Wilson ratio $\sim\chi T/C$. A FL-like saturation of this estimated susceptibility is then obtained in CePtSi below 1 K, whereas in $CePtSi_{0.9}Ge_{0.1}$ a NFL-like divergent behavior remains at low temperatures.

From fits to the susceptibility data, we find that the Kondo-disorder and Griffiths phase models give similar predictions of the spread of the local susceptibilities in both materials, and that the disorder in the susceptibility can account for the observed NMR line broadening in both CePtSi and $CePtSi_{0.9}Ge_{0.1}$. The inclusion of the estimated susceptibility data in the fits to the disorder-driven models gives a narrower distribution of susceptibilities in CePtSi than in $CePtSi_{0.9}Ge_{0.1}$, which allows Fermi-liquid behavior in

CePtSi and also accounts for the NFL behavior in $CePtSi_{0.9}Ge_{0.1}$. However, the Kondo-disorder and Griffiths models cannot be distinguished in our NMR linewidth study. A study of spin dynamics using nuclear spin-lattice relaxation measurements may be useful in this regard, and is currently in progress.

The article is organized as follows: Sec. II describes the calculation of the single-ion CEF susceptibility (and its modification by the $s-f$ exchange interaction) and the disorder-driven NFL models. Then the disorder in the magnetic susceptibility is estimated. A description of the NMR experiments is given in Sec. III, where the NMR linewidth and line shape are analyzed. The applicability of the disorder-driven NFL models to $CePtSi_{1-x}Ge_x$ is discussed in Sec. IV. Then Sec. V gives our conclusions.

II. SPATIAL DISTRIBUTION OF LOCAL MAGNETIC SUSCEPTIBILITIES

The Kondo-disorder[10,11] and Griffiths phase[12,13] models are the two major disorder-driven NFL models to approach the NFL problem from the point of view of structural disorder effects. The Kondo-disorder model is based on single-ion Kondo physics. The effect of lattice disorder is to produce an inhomogeneous environment (magnetic disorder) such that the strength of the Kondo interaction between the local moment and the conduction electrons, i.e., the local Kondo temperature T_K, is spatially distributed. The local moments which are not quenched by the conduction electrons, because T_K is lower than the sample temperature, can therefore prevent the system from returning to FL behavior at even very low temperatures if there is enough disorder. In contrast to the Kondo-disorder model, the RKKY interaction between local moments as well as the Kondo effect are considered in the Griffiths phase model. The combination of disorder and the competition between the RKKY and Kondo interactions can lead to an inhomogeneous environment equivalent to a so-called Griffiths phase[34] characterized by rare strongly coupled magnetic clusters which dominate the NFL physics.

Despite a marked difference in mechanisms, the essential idea of both models is to assume the coexistence of two electronic systems caused by the structural disorder. One of the systems is in a metallic (Fermi-liquid like) phase, and the other one is in a magnetic phase (unquenched local moments or magnetic clusters). This kind of inhomogeneous environment therefore gives a route to NFL behavior at low temperatures.

As mentioned above, magnetic ions in many heavy-fermion (or Kondo) systems behave like isolated ions, i.e., the intra-site Kondo interaction is much stronger than the intersite RKKY interaction, even in dense Kondo systems. The evidence for this in CePtSi and $CePtSi_{0.9}Ge_{0.1}$ can be seen from the Ce^{3+} effective moments at high temperatures, 2.56 μ_B/Ce and 2.48 μ_B/Ce, respectively, which are tolerably close to the free-ion value 2.54 μ_B/Ce.[35] This suggests that the bulk susceptibility can be described in terms of single-ion susceptibilities of the Ce^{3+} ions.

The Kondo-disorder and Griffiths phase models provide different forms of the distribution function for the disorder-induced inhomogeneous local susceptibility. If the expression for the single-ion susceptibility is known, by doing least-square fits of the bulk susceptibility $\chi_{\text{bulk}}(T)$ to the single-ion susceptibility $\chi(T)$ averaged over the distribution function $P(\chi)$ from the disorder models $[\chi_{\text{bulk}}(T) = \int_0^\infty \chi(T)P(\chi)d\chi]$, the parameters in the distribution functions can be obtained, and the amount of the magnetic disorder in the materials can be estimated.

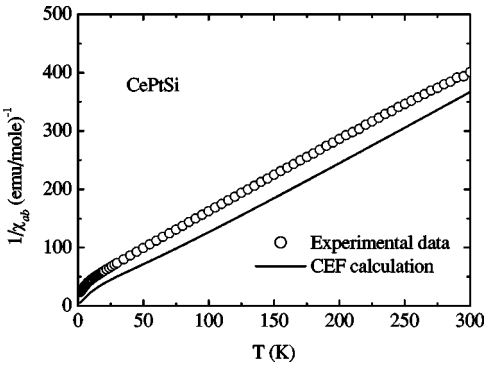

FIG. 2. A plot of the inverse *ab*-plane susceptibility versus temperature for CePtSi. The circles denote the experimental data, and the curve is obtained from the crystalline electric field (CEF) calculation.

A. Single-ion susceptibility

The magnetic susceptibility in a Kondo system can be roughly described by a Curie-Weiss law or a Brillouin function for the magnetization with the temperature T replaced by $(T+\alpha T_K)$, where α is a constant of order unity.[36] Figure 2 shows a plot of the inverse *ab*-plane susceptibility $1/\chi_{ab}$ versus temperature for CePtSi. Downward curvature is seen at low temperatures, which is not expected from a Curie-Weiss law or saturation of a Brillouin function. Two possible mechanisms may explain this curvature (assuming no paramagnetic Ce^{3+} impurity in samples): CEF splitting and magnetic disorder.

The downward curvature suggests that the effective moment is reduced at low temperatures, because the slope of a $1/\chi$ plot is inversely proportional to square of the effective moment. If the CEF effect is strong enough, the Ce^{3+} ($J=5/2$) sixfold degeneracy will be removed. From inelastic neutron scattering (INS) experiments,[32] we know there is a strong CEF effect in CePtSi and the ground state is a doublet. Therefore fewer CEF-split levels contribute to the susceptibility at low temperatures than at high temperatures, leading to a reduced low-temperature effective moment. On the other hand, if there is significant disorder, according to the disorder-driven NFL theories, because of the existence of the magnetic phase, the bulk (averaged) susceptibility is enhanced at low temperatures when compared with the ordered case. Thus the $1/\chi$ plot can exhibit a downward curvature due to this disorder.

Clearly, a simple Curie-Weiss or Brillouin function is not a suitable single-ion susceptibility expression for $CePtSi_{1-x}Ge_x$ because of CEF effects. Since the downward

curvature may be a combination of CEF and disorder effects, the CEF splitting needs to be considered in deriving the single-ion susceptibility expression in order to avoid overestimating the disorder in $CePtSi_{1-x}Ge_x$.

A Ce^{3+} ion in CePtSi experiences a tetragonal crystal field, which splits the $J=5/2$ multiplet into three doublets. The energy levels and states (three doublets) are conventionally expressed as[37]

$$E_1,\ |\Gamma_6(\pm)\rangle = |\pm 1/2\rangle,$$

$$E_2,\ |\Gamma_7^{(1)}(\pm)\rangle = a|\pm 5/2\rangle + \sqrt{1-a^2}|\mp 3/2\rangle,$$

$$E_3,\ |\Gamma_7^{(2)}(\pm)\rangle = \sqrt{1-a^2}|\pm 5/2\rangle - a|\mp 3/2\rangle, \qquad (1)$$

where E_1, E_2, and E_3 are the eigenvalues of the eigenstates $|\Gamma_6(\pm)\rangle$, $|\Gamma_7^{(1)}(\pm)\rangle$, and $|\Gamma_7^{(2)}(\pm)\rangle$, respectively, and a is a CEF parameter. From inelastic neutron scattering experiments,[32] $a=0.63$ and $|\Gamma_7^{(1)}(\pm)\rangle$ is found to be the ground state. The excited states are $|\Gamma_6(\pm)\rangle$ and $|\Gamma_7^{(2)}(\pm)\rangle$ with energies $E_1=6.3$ meV and $E_3=17.8$ meV, respectively.

The free-ion susceptibility due to the CEF splitting can be calculated using the degenerate perturbation method, if the applied magnetic field is small enough (<1 T in our study). The resulting expression can be found in Ref. 38. Figure 2 gives a comparison of $1/\chi_{ab}$ versus temperature between the experimental data and the CEF free-ion susceptibility calculated using the CEF parameters obtained from the INS experiments. Surprisingly, the measured curve shows a similar curvature as the CEF calculated curve, except there is a shift between them. Similar behavior has been observed in $Ce_{0.06}La_{0.94}Cu_{2.05}Si_2$.[38] The shift in the temperature scale is attributed to the $s-f$ exchange interaction between the magnetic ion and the conduction electrons, which is not included in the CEF calculation. This exchange interaction gives rise to both the Kondo effect and the RKKY interaction. Its effect on the susceptibility can be crudely modeled by a scaling temperature Δ in the simple Curie-Weiss expression. The Kondo temperatures in CePtSi and $Ce_{0.06}La_{0.94}Cu_{2.05}Si_2$ are around 10 K, which is much smaller than the CEF splitting.[38,39] This may explain why the observed $1/\chi_{ab}$ curve is shifted, but keeps essentially the same curvature as in the CEF calculated free-ion curve.

The combined effect of the exchange interaction and crystal fields is very complicated, and to our knowledge no analytic expression for the susceptibility has been derived for this problem over the entire temperature range. We have therefore assumed the simple form

$$\chi(T;\Delta) = \eta\chi_{\mathrm{CEF}}(T+\Delta) + \chi_0 \qquad (2)$$

for the single-ion susceptibility, where χ_{CEF} is the CEF susceptibility, η is a reduction factor due to the spin polarization of the conduction electrons,[40] and χ_0 is the Pauli susceptibility. Equation (2) takes into account the effects of the exchange interaction (via Δ) and the CEF (via the form of χ_{CEF}). Hence we can roughly estimate how the local susceptibility is distributed in $CePtSi_{1-x}Ge_x$ by distributing the single-ion susceptibility according to the disorder-driven NFL models. The origin of the inhomogeneous distribution of the local susceptibilities comes from the disorder-induced spread of the local energy scales Δ. By fitting the bulk susceptibility to the function

$$\chi_{\mathrm{bulk}}(T) = \int_0^\infty \chi(T;\Delta)P(\Delta)d\Delta, \qquad (3)$$

where $P(\Delta)$ is the distribution function for the energy scale Δ, the distribution of the local susceptibilities can be obtained.

B. Kondo-disorder model

In the Kondo-disorder model the local energy scale Δ corresponds to the Kondo energy scale T_K ($\Delta=T_K$), which is distributed over the sample. Generally T_K is related to the Zener coupling constant $g=\rho(\varepsilon_F)\mathcal{J}$ by $T_K=\varepsilon_F e^{-1/|g|}$, where ε_F is the Fermi energy, $\rho(\varepsilon_F)$ is the conduction electron density of states, and $\mathcal{J}$ is the exchange coupling constant. Because the coupling strength is very sensitive to the distance between the f ion and conduction electrons, modest lattice disorder can produce a significant spatial distribution of the coupling constants g over the sample. A small variation of g then leads to a wide spread of the Kondo temperatures due to the exponential dependence of T_K on g. Local environment disorder may also have an influence on the crystalline electric field, and produce a variation in the CEF levels. Since the effect of disorder on the CEF is likely to be relatively small compared with the disorder in the coupling constant, for simplicity only the latter is considered.

Due to the lack of understanding of how the coupling constant is spatially distributed over the sample, in practice we have assumed that the coupling constant has a Gaussian distribution with average $\overline{g}$ and width δg: $P(g)=\exp[-(g-\overline{g})^2/2\delta g^2]/(\sqrt{2\pi}\delta g)$. The distribution function of Kondo temperatures $P(T_K)$ is then given by

$$P(T_K) = P(g)|dg/dT_K|. \qquad (4)$$

If the disorder is strong enough, it is possible to have $P(T_K\rightarrow 0)\neq 0$, which means that some of the local moments are not quenched by the Kondo effect at any finite temperature. These unquenched moments therefore prevent the system from returning to Fermi-liquid behavior at very low excitation energy.

C. Griffiths phase model

The Griffiths phase model has a similar disorder approach to the NFL problem. The disorder generates an inhomogeneous environment in which some f moments are quenched by the Kondo interaction and some are not. The unquenched moments are coupled by the long-range RKKY interaction and form magnetic clusters. The largest of these strongly coupled clusters dominate the low temperature physics, and a broad distribution of the local susceptibilities is also expected.

In this model the spin-flip of a cluster is described as a tunneling process in a two-level system. The local energy scale Δ is given by the tunneling energy E.[25] Because of

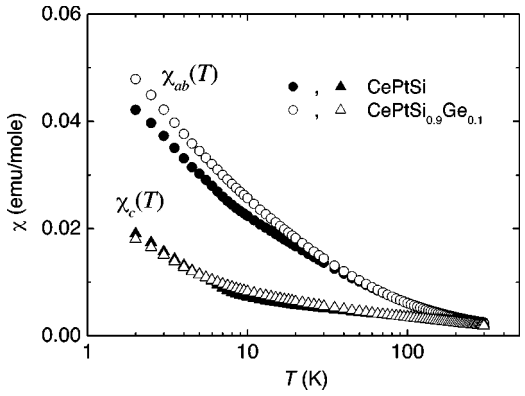

FIG. 3. Temperature dependence of the bulk susceptibilities in CePtSi (filled symbols) and $CePtSi_{0.9}Ge_{0.1}$ (open symbols). Triangles: the *c*-axis susceptibilities. Circles: the *ab*-plane susceptibilities.

disorder, the energy E is distributed over the sample with a cut-off energy ϵ_0,

$$P(E) = \begin{cases} \frac{\lambda}{\epsilon_0}\left(\frac{E}{\epsilon_0}\right)^{-1+\lambda}, & 0 < E < \epsilon_0, \\ 0, & E > \epsilon_0, \end{cases} \quad (5)$$

where $0 \leqslant \lambda \leqslant 1$ characterizes the low temperature properties in a Griffiths phase. If $\lambda < 1$, the susceptibility and specific heat diverge at zero temperature, and NFL behavior occurs because of the Griffiths singularity. The marginal case $\lambda = 1$ also leads to logarithmic singularities as in the Kondo-disorder approach.[13]

D. Sample preparation and susceptibility analysis

1. Samples

Samples of CePtSi and $CePtSi_{1-x}Ge_x$ were prepared by arc melting and annealed for 110 h at 1050 °C. The sample quality has been examined by x-ray powder diffraction, which shows only single phase structure. The polycrystalline ingot samples were pulverized into powder with particle size smaller than 75 μm for two reasons. One is that particles smaller than the rf skin depth allow NMR rf pulses to penetrate the samples. The other reason is that single-crystal powder grains allow use of the field alignment technique[41,42] to align the powders for measurements of anisotropic properties.

2. Magnetic susceptibility

The temperature dependence of the dc magnetic susceptibility was originally measured in CePtSi and $CePtSi_{0.9}Ge_{0.1}$ between 2 and 300 K with a commercial SQUID magnetometer. Figure 3 presents the anisotropic susceptibilities measured in the field-aligned powder samples of CePtSi (filled circles and triangles) and $CePtSi_{0.9}Ge_{0.1}$ (open circles and triangles). The susceptibilities for field in the *ab* plane (circles) are larger than for field along the *c* axis (triangles), and the anisotropy increases as the temperature decreases. Since the strongest NMR line broadening is also observed for the NMR field perpendicular to the *c* axis for both samples (see Sec. III), most of our analysis uses susceptibility and NMR data taken with field applied in this direction.

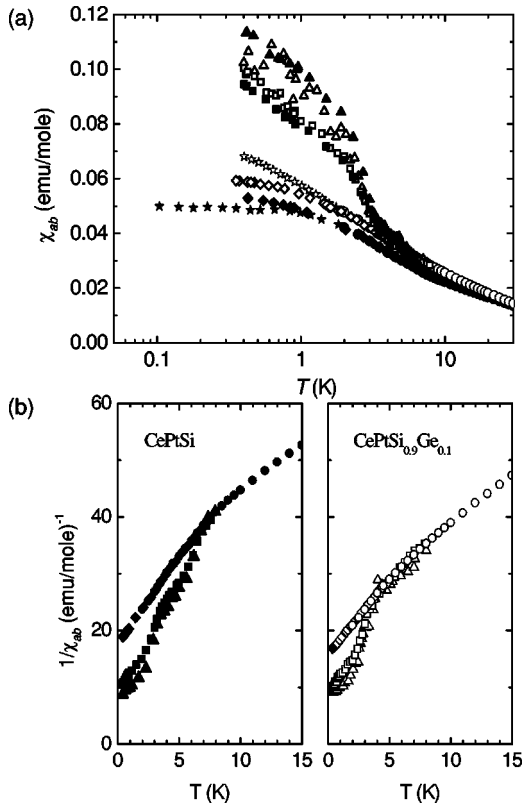

FIG. 4. (a) *ab*-plane susceptibilities in CePtSi (filled symbols) and $CePtSi_{0.9}Ge_{0.1}$ (open symbols). Triangles: low temperatures (T=0.4–8 K), applied fields 0.05 T and 0.01 T for CePtSi and $CePtSi_{0.9}Ge_{0.1}$, respectively. Squares: low temperatures, 0.1 T and 0.05 T for CePtSi and $CePtSi_{0.9}Ge_{0.1}$, respectively. Diamonds: low temperatures, 0.5 T. Circles: $T > 2$ K, 0.5 T. Stars: estimated susceptibility from extrapolated Wilson ratio (see text). (b) Inverse susceptibilities of CePtSi and $CePtSi_{0.9}Ge_{0.1}$.

To our knowledge, evidence for FL and NFL behavior in CePtSi and $CePtSi_{0.9}Ge_{0.1}$, respectively, is only found in specific heat measurements for temperatures below 1 K.[30,33] We therefore used a Faraday balance magnetometer which is integrated with a ^{3}He refrigerator for magnetization measurements below 2 K. The results of low-temperature *ab*-plane susceptibilities in CePtSi (filled symbols) and $CePtSi_{0.9}Ge_{0.1}$ (open symbols) are given in Fig. 4. The magnetization has been measured at several different external magnetic fields in the temperature range of 0.4–8 K. The susceptibilities of both samples show obvious field dependencies for temperatures below 5 K: the low-temperature susceptibility saturates at high magnetic fields. Since this field dependence is not expected for a Kondo paramagnetic metal, we suspect that spurious magnetic phases may exist in these samples. Figure 4(b) gives plots of inverse susceptibility versus temperature, where CePtSi shows an additional inflection point at 7 K more obvious than $CePtSi_{0.9}Ge_{0.1}$. We found that our $1/\chi$ plots show similar field dependence as the one reported by Köhler *et al.*,[43] except for the additional inflection point in our CePtSi sample. They concluded that the field dependence

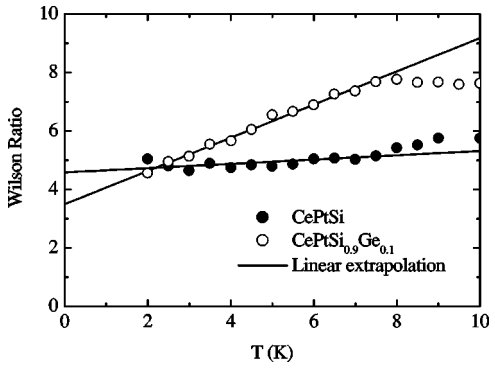

FIG. 5. Wilson ratios at low temperatures in CePtSi (filled circles) and $CePtSi_{0.9}Ge_{0.1}$ (open circles). The straight lines denote the linear extrapolations.

in magnetization is probably due to a ferromagnetic spurious phase, and that this might be expected because $CePtSi_{1-x}Ge_x$ is near a magnetic stability; its ground state could be sensitive to disorder in the material. Since a Curie tail (rather than complete saturation[43]) is also visible in Fig. 4(a), we think that both paramagnetic and ferromagnetic Ce^{3+} impurities might exist.

3. Wilson ratio

Due to the presence of impurity phases, it is difficult to separate the impurity-phase contribution in order to obtain the intrinsic susceptibility of $CePtSi_{1-x}Ge_x$. To bypass this difficulty, we have calculated the Wilson ratio $R=(\pi^2 k_B^2/3\mu_{\rm eff}^2)\chi T/C$, where $\mu_{\rm eff}$ is the effective magnetic moment, using our susceptibility data and specific heat data (from Refs. 30 and 33) above 2 K. Then the susceptibility below 2 K can be estimated from specific heat data in this temperature range and the extrapolated Wilson ratio. (The free-ion value $\mu_{\rm eff}=2.54\ \mu_B$/Ce has been used in the Wilson ratio, although the estimated χ is independent of this choice.)

Figure 5 gives the temperature dependence of the Wilson ratio at low temperatures for CePtSi (filled circles) and $CePtSi_{0.9}Ge_{0.1}$ (open circles). CePtSi shows a relatively constant Wilson ratio below 8 K in agreement with the FL

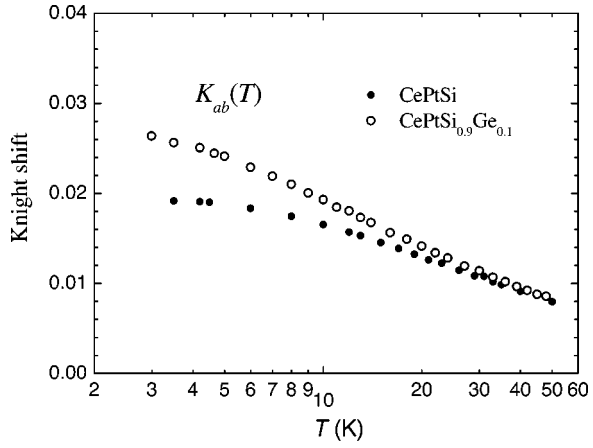

FIG. 6. The temperature dependence of NMR Knight shifts in CePtSi (filled circles) and $CePtSi_{0.9}Ge_{0.1}$ (open circles).

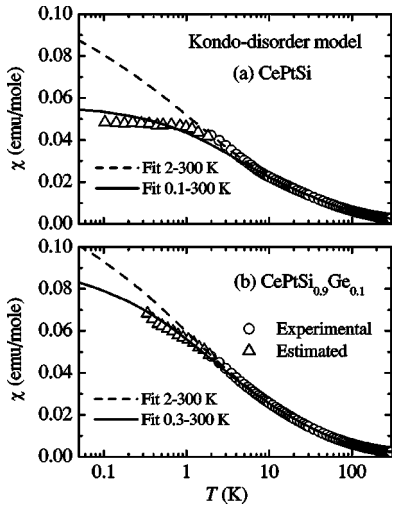

FIG. 7. Susceptibility fits to the Kondo-disorder model in (a) CePtSi and (b) $CePtSi_{0.9}Ge_{0.1}$. Circles: experimental data. Triangles: estimated data. Dashed curves: fits for only the experimental data from 2 to 300 K. Solid curves: fits for the entire susceptibilities including the estimated data below 2 K.

theory, although the ratio is a little higher than the universal value $R=2$ in a Kondo system.[44] This may be due to the fact that the *ab*-plane instead of the isotropic susceptibility is used in the calculation, or to the choice of the effective moment $\mu_{\rm eff}$. The Wilson ratio in $CePtSi_{0.9}Ge_{0.1}$ shows a linear relation with temperature below 8 K, which is not expected for a typical FL system but is similar to that predicted from the Kondo-disorder model.[11]

Linear extrapolations of the Wilson ratios to low temperatures in Fig. 5 (straight lines) are used to estimate the susceptibility below 2 K from the specific heat data of Refs. 30 and 33. These estimated values of χ are shown in Fig. 4(a) for CePtSi (filled stars) and $CePtSi_{0.9}Ge_{0.1}$ (open stars), respectively. Below 2 K, CePtSi shows a temperature-independent susceptibility (FL like), whereas $CePtSi_{0.9}Ge_{0.1}$ has a roughly logarithmic temperature dependence (NFL like). Although the accuracy of this extrapolation procedure cannot be guaranteed, the relatively smooth linear temperature dependence of the Wilson ratios (Fig. 5) and the reproducible FL and NFL behavior in the estimated susceptibilities of CePtSi and $CePtSi_{0.9}Ge_{0.1}$, respectively, suggest that the estimated susceptibilities are reasonably acceptable. This method for estimating the susceptibility is supported by the NMR Knight shift data for $T\gtrsim 3$ K given in Fig. 6. The Knight shift K in a metal is proportional to the local spin susceptibility: $K=A\chi$, where A is the hyperfine coupling constant, as discussed in Sec. III. Spurious phases often occupy a small volume fraction or have very different Knight shifts, in which case the bulk shift accurately reflects the pure local susceptibility. Figure 6 shows that down to ~ 3 K the Knight shifts in CePtSi and $CePtSi_{0.9}Ge_{0.1}$ do indeed exhibit the expected FL- and NFL-like behavior, respectively.

4. Susceptibility fits to disorder models

Figures 7(a) and 7(b) give least-square fits of the *ab*-plane susceptibilities in CePtSi and $CePtSi_{0.9}Ge_{0.1}$, respectively, to

TABLE I. Fit parameters in the Kondo-disorder model fits for CePtSi and $CePtSi_{0.9}Ge_{0.1}$ in the temperature ranges from 2 to 300 K and 0.1 (or 0.3) to 300 K (see text). Here E_1, E_2, E_3, and a are CEF parameters, η is a reduction factor, and $\bar{g}$ and δg are the average and the spread of the coupling constants g, respectively.

	E_1 (meV)	E_2	E_3 (meV)	a	η	$\bar{g}$	δg
CePtSi							
2–300 K	6.3(3)	0	18(5)	0.64(6)	0.81(4)	0.138(4)	0.019(3)
0.1–300 K	6.3	0	18	0.64	0.81	0.1387(2)	0.0139(3)
$CePtSi_{0.9}Ge_{0.1}$							
2–300 K	3.3(7)	0	18(2)	0.79(4)	0.859(9)	0.135(2)	0.018(2)
0.3–300 K	3.3	0	18	0.79	0.859	0.1355(1)	0.0164(1)

the Kondo-disorder model as described in Sec. II B. The dashed curves represent the fits for only the measured susceptibility data from 2 to 300 K, which agree with the experimental data very well. Table I lists the obtained fit parameters. For CePtSi the CEF parameters from our fit are very close to the values ($E_1=6.3$ meV, $E_2=0$, $E_3=17.8$ meV, and $a=0.63$) obtained from the INS experiments.[32] The factors η for both samples are less than one as expected. The deviation in the CEF parameters E_1 and a in $CePtSi_{0.9}Ge_{0.1}$ from the values in CePtSi are not surprising because the local electric field may be modified due to the Ge doping.

However, the fit curves extended below 2 K do not follow the estimated data very well especially for CePtSi. This indicates that inclusion of the estimated data below 2 K for the fits is necessary. The solid curves in Fig. 7 are the susceptibility fits to the Kondo-disorder model over the entire temperature range (with the CEF parameters fixed at the values found from INS data[32]). Only the average coupling constant $\bar{g}$ and the distribution width δg are varied for best fit, which gives $\bar{g}=0.1387(2)$, $\delta g=0.0139(3)$ for CePtSi and $\bar{g}=0.1355(1)$, $\delta g=0.0164(1)$ for $CePtSi_{0.9}Ge_{0.1}$.[45] The new values of $\bar{g}$ are similar to those listed in Table I for both samples, whereas there is a strong reduction in δg for CePtSi in order to describe the saturated susceptibility at low temperatures. A slightly reduced δg is obtained for $CePtSi_{0.9}Ge_{0.1}$, but it is still within the uncertainty of the previous susceptibility fit above 2 K. However, for CePtSi there is an appreciable discrepancy between the fit curve [solid curve in Fig. 7(a)] and the susceptibility data. The fit does not improve significantly even if the CEF parameters are free to change, and in this case the obtained CEF fit parameters do not agree with those from INS experiments.

One possible cause of the imperfect fit of the Kondo-disorder model in CePtSi could be the breakdown of Eq. (2) as an accurate model of the single-ion Kondo susceptibility. In the conventional Kondo problem the high-temperature susceptibility can be described well by a Curie-Weiss law, whereas $\chi(T)=\chi(0)[1-c(T/T_K)^2]$, $c\sim 1$, at very low temperatures where FL theory is valid.[36] Therefore the single-ion susceptibility expression [Eq. (2)] based on a Curie-Weiss-type *ansatz* will not be accurate at low temperatures. If the disorder effect is strong enough, Eq. (2) is still expected to be a reasonable approximation even at low temperatures, but this will not be the case for weak disorder.

The spread of the new coupling constants δg is found to be close in both samples: the ratio $\delta g/\bar{g}=0.1$ in CePtSi is only a little smaller than $\delta g/\bar{g}=0.12$ in $CePtSi_{0.9}Ge_{0.1}$. The fits to the Kondo-disorder model predict, therefore, that disorder in the stoichiometric compound CePtSi and the 10% Ge doped sample are comparable, which is unexpected considering the evidence for Fermi-liquid behavior in CePtSi. We return to this point below in Sec. IV.

Results of a similar treatment of the susceptibility fits to the Griffiths phase model are shown in Fig. 8. The dashed curves in Figs. 8(a) and 8(b) are the fits for the measured susceptibilities above 2 K, which again deviate from the estimated susceptibilities below 2 K for both CePtSi and $CePtSi_{0.9}Ge_{0.1}$. The fit parameters are listed in Table II. We find that for the fits of the experimental data between 2 and 300 K, the CEF parameters (E_1, E_2, E_3, and a) agree with the inelastic neutron scattering data, and η has a similar value as in the Kondo-disorder model case.

The solid curves in Fig. 8 are the susceptibility fits to the Griffiths phase model over the entire temperature range with the CEF parameters fixed at the INS values and with λ and ϵ_0 as fit parameters. Similar to the fits of the Kondo-disorder

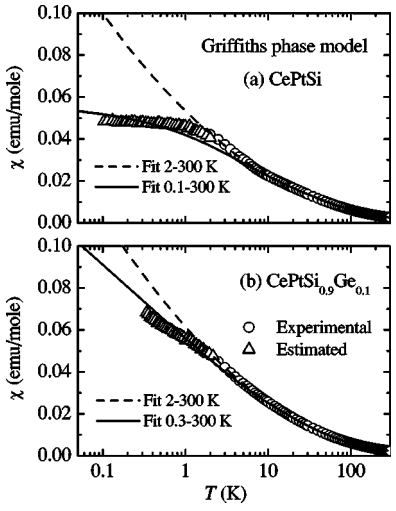

FIG. 8. Susceptibility fits to the Griffiths phase model in (a) CePtSi and (b) $CePtSi_{0.9}Ge_{0.1}$. Circles: experimental data. Triangles: estimated data. Dashed curves: fits for only the experimental data from 2 to 300 K. Solid curves: fits for the entire susceptibilities including the estimated data below 2 K.

TABLE II. Fit parameters in the Griffiths phase model fits for CePtSi and $CePtSi_{0.9}Ge_{0.1}$ in the temperature ranges from 2 to 300 K and 0.1 (or 0.3) to 300 K (see text). Here E_1, E_2, E_3, and a are CEF parameters, η is a reduction factor, and λ and ϵ_0 are the critical exponent and the cut-off energy, respectively, in the Griffiths phase model.

	E_1 (meV)	E_2	E_3 (meV)	a	η	λ	ϵ_0
CePtSi							
2–300 K	6.3(2)	0	18(1)	0.66(2)	0.81(1)	0.86(8)	22(2)
0.1–300 K	6.3	0	18	0.66	0.81	1.51(4)	15.3(4)
$CePtSi_{0.9}Ge_{0.1}$							
2–300 K	3.7(7)	0	20(3)	0.77(4)	0.85(1)	0.88(9)	18(2)
0.3–300 K	3.7	0	20	0.77	0.85	1.01(1)	17.3(1)

model, the Griffiths phase model does not fit the low-temperature susceptibility data well in CePtSi. The new fit values are $\lambda=1.51(4)$, $\epsilon_0=15.3(4)$ for CePtSi, and $\lambda=1.01(1)$, $\epsilon_0=17.3(1)$ for $CePtSi_{0.9}Ge_{0.1}$. According to the Griffiths phase model, the values of $\lambda>1$ in CePtSi and $\lambda\approx1$ in $CePtSi_{0.9}Ge_{0.1}$ suggest FL and NFL behavior, respectively, and agree with the specific heat measurements, as expected. These experimental results will be discussed further in Sec. IV.

III. NMR EXPERIMENTS

Experimentally structural disorder and induced magnetic disorder have been studied by various techniques such as resistivity measurements, XAFS experiments,[26] elastic neutron diffraction,[46] NMR,[10] and μSR.[23] Since disorder-driven NFL models predict that structural disorder can produce magnetic disorder in the NFL systems, NMR is a good technique to study the local static and dynamic properties of a disordered magnetic environment. A NMR study of the static properties of $CePtSi_{1-x}Ge_x$ is reported in this paper. Nuclear spin relaxation experiments to investigate spin dynamics are in progress and will be reported later.

The frequency shift and the distribution of the shifts (i.e., line broadening) in a NMR spectrum can provide information on the magnetic interactions between the probe nucleus and its surrounding environment. The NMR frequency shift (Knight shift) K of a nucleus is associated with neighboring local moments by[47]

$$K=\sum_{j=1}^{n} a_j\chi_j, \tag{6}$$

where a_j is the hyperfine coupling constant, n is the number of f ions that interact with the probe nucleus, and χ_j is the susceptibility of the jth local moment. Clearly, from this relation any disorder in the local susceptibility will result in a spread of NMR frequency shifts. The structural disorder can cause a distribution of the hyperfine coupling constants a_j as well, which also contributes a spread to the frequency shifts. The contributions to the line broadening from the spreads of local susceptibilities and hyperfine coupling constants can be determined separately if the former has a temperature dependence (caused by the temperature-dependent susceptibility), but the latter is constant. Our NMR data show that most of the line broadening comes from disorder in the local susceptibility.

The NMR spectra were obtained using a standard field-swept pulsed NMR technique, with the spin-echo signals processed using the frequency-shifted-and-summed Fourier-transform technique.[48] A typical powder-pattern spectrum in ^{29}Si obtained from an unaligned CePtSi powder sample is shown in Fig. 9 (solid curve). The inhomogeneous broadening is caused in part by the anisotropic Knight shift and in part by the susceptibility inhomogeneity. Thus it is not easy to extract the information on the magnetic disorder from this type of spectrum. In order to eliminate the anisotropic "powder-pattern" broadening, the magnetic field alignment technique has been applied to prepare aligned samples CePtSi and $CePtSi_{0.9}Ge_{0.1}$. Since both samples have the largest magnetic susceptibility in the basal plane, a rotational alignment method[41] has been used, so that the c axes in the single-crystal powder grains are all aligned parallel to the rotation axis and the a and b axes are randomly distributed in the plane perpendicular to the rotation axis.

The dotted and dashed-dotted curves in Fig. 9 are spectra obtained in the aligned CePtSi powder sample for the NMR

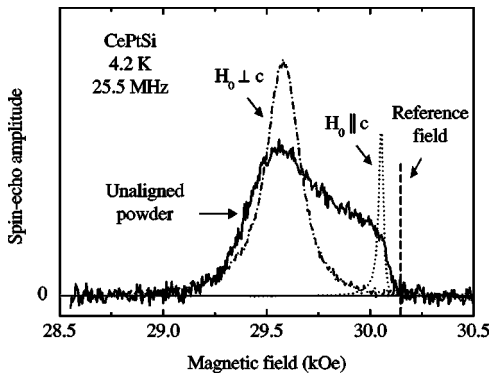

FIG. 9. ^{29}Si NMR spectra for the unaligned (solid curve) and aligned (dotted and dashed-dotted curves) CePtSi powder samples at 4.2 K and at a frequency of 25.5 MHz. Dotted and dashed-dotted curves are for spectra with the NMR field $\mathbf{H}_0$ directed parallel and perpendicular to the crystal c axis, respectively. The reference field is the unshifted resonance field at 30.145 kOe=25.5 MHz/$(\gamma/2\pi)$, where $\gamma/2\pi=0.8458$ MHz/kOe is the ^{29}Si nuclear gyromagnetic ratio.

field $\mathbf{H}_0$ directed parallel and perpendicular to the c axis, respectively. There is extra line broadening for $\mathbf{H}_0 \perp \mathbf{c}$. The observed broadening suggests disorder in the local susceptibility, similar to that observed in $CeRuRhSi_2$.[25]

Susceptibility measurements discussed in Sec. II D show that CePtSi and $CePtSi_{0.9}Ge_{0.1}$ have strong magnetic anisotropy; the ab plane has a much greater Curie-Weiss-type susceptibility than the c axis. Therefore if there is any disorder in the susceptibility, it will be easier to see the temperature-dependent line broadening with $\mathbf{H}_0$ in the ab plane rather than along the c axis. Since for $\mathbf{H}_0 \perp \mathbf{c}$ the spectra show pronounced line broadening and a strong Curie-Weiss-type temperature-dependent susceptibility, all NMR spectra discussed below have been taken for $\mathbf{H}_0 \perp \mathbf{c}$.

A. NMR linewidth

Since the frequency shift is linearly dependent on the local susceptibility [Eq. (6)], any spatial distribution of the susceptibilities is reflected in a spread of the frequency shifts (NMR linewidth). A quantitative estimate of the spread is the rms value of the Knight shift spread δK obtained from the NMR linewidth.

Starting from Eq. (6), the spatial average of the Knight shift $\overline{K}$ can be shown to be given by

$$\overline{K} = a\overline{\chi}, \quad a \equiv \sum_j^n a_j, \tag{7}$$

where the bar stands for a spatial average. Assuming no correlation between disorder in the hyperfine coupling constant a_j and the susceptibility χ_j, the rms value of the Knight shift spread δK can be written as[49]

$$\overline{\delta K^2} \equiv \overline{(K-\overline{K})^2} = \sum_{j,k} (\overline{a_j a_k})(\overline{\delta\chi_j \delta\chi_k}) + \left(\sum_{j,k} \overline{\delta a_j \delta a_k}\right)\overline{\chi}^2, \tag{8}$$

where $\delta a_j \equiv a_j - \overline{a_j}$ and $\delta\chi_{j,k} \equiv \chi_{j,k} - \overline{\chi_{j,k}}$. Disorder in the hyperfine coupling constant is included in this expression (the second term).

The correlation term $\overline{\delta\chi_j \delta\chi_k}$ can be simplified by considering the two extreme limits: long-range correlation (LRC) and short-range correlation (SRC). In the LRC limit, the correlation length between the local moments is much longer than the lattice constant and $\overline{\delta\chi_j \delta\chi_k} \approx \overline{\delta\chi^2}$, where $\overline{\delta\chi^2} \equiv \overline{\chi^2} - \overline{\chi}^2$ is the mean-square width of the susceptibility distribution. Whereas in the SRC limit, the local moment is correlated only over a range much smaller than a lattice constant, such that to a first approximation $\overline{\delta\chi_j \delta\chi_k} \approx \overline{\delta\chi^2}\delta_{jk}$. It should be noted that this correlation is an effect of structural disorder, and is unrelated to critical spatial correlation.

In order to obtain a simple expression for the relation between the spread of the Knight shifts $\delta K \equiv (\overline{\delta K^2})^{1/2}$ and the spread of local susceptibilities $\delta\chi \equiv (\overline{\delta\chi^2})^{1/2}$, we introduce a model in which an effective number n_{eff} of f-ion near neighbors are coupled to the NMR probe nucleus by an effective hyperfine coupling constant a_{eff}. Then from Eq. (7), $a \approx n_{\text{eff}} a_{\text{eff}}$. In the SRC and LRC correlation limits, as described in Ref. 49, the relative spread $\delta K/\overline{K}$ is found to have a simple relation to the ratio $\delta\chi/\overline{\chi}$ (the spread of the susceptibility $\delta\chi$ to the bulk susceptibility $\overline{\chi}$):

$$\frac{\delta K}{\overline{K}} = \begin{cases} [(\delta\chi/\overline{\chi})^2 + A]^{1/2}, & \text{LRC} \\ \left[\dfrac{1}{n_{\text{eff}}}(\delta\chi/\overline{\chi})^2 + A\right]^{1/2}, & \text{SRC} \end{cases} \tag{9}$$

where the constant A is a temperature-independent term which comes from the disorder in the hyperfine coupling constant a_{ij}.

In the disorder-driven NFL models, the ratio $\delta\chi/\overline{\chi}$ is strongly dependent on temperature. It tends to increase at low temperatures, and is predicted to have a roughly linear relation with $\overline{\chi}$, i.e., $\delta\chi/\overline{\chi} \propto \overline{\chi}$. Equation (9) shows that the spread of the NMR frequency shifts can be due to disorder effects in both the local susceptibility and the hyperfine coupling constant. The former is temperature dependent and the latter is not. In a plot of $(\delta K/\overline{K})^2$ versus $(\overline{\chi})^2$, the effect of A is to produce a nonzero intercept, so that it can be separated from the susceptibility contribution.

^{29}Si NMR spectra have been obtained for the NMR field $\mathbf{H}_0 \perp \mathbf{c}$ axis in both CePtSi and $CePtSi_{0.9}Ge_{0.1}$ at a NMR frequency of 25.5 MHz from 2 to 50 K. ^{195}Pt NMR spectra also have been measured in $CePtSi_{0.9}Ge_{0.1}$. These spectra are described better by a Lorentzian than a Gaussian function. Unfortunately, the second moment of a Lorentzian is not well defined, and the rms value of the linewidth cannot be determined directly. Therefore the half width at half maximum (HWHM) has been used to characterize the NMR linewidths. The use of HWHM still can offer a good estimate of the rms linewidth because the HWHM linewidth from the Lorentzian fit is found to be close to the rms width of the disorder-driven theoretical line discussed in Sec. III B below.

The ^{29}Si $\overline{K}$ and δK data, plotted as functions of ab-plane bulk susceptibility χ with temperature an implicit parameter, are shown in Fig. 10. CePtSi and $CePtSi_{0.9}Ge_{0.1}$ show very similar behavior. The distribution width of the Knight shifts increases rapidly at large susceptibilities (low temperatures) compared with the average Knight shift, which strongly sug-

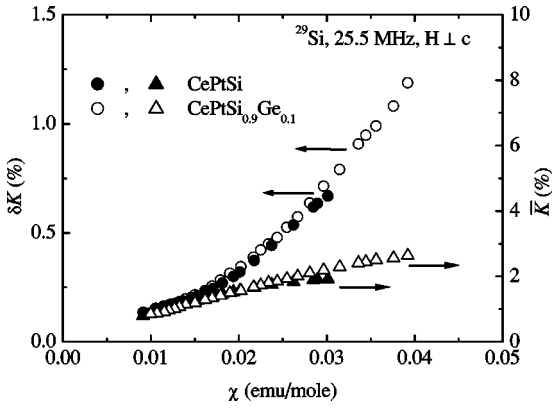

FIG. 10. Plots of ^{29}Si NMR Knight shift $\overline{K}$ and the distribution width of the Knight shifts δK as functions of susceptibility in CePtSi and $CePtSi_{0.9}Ge_{0.1}$.

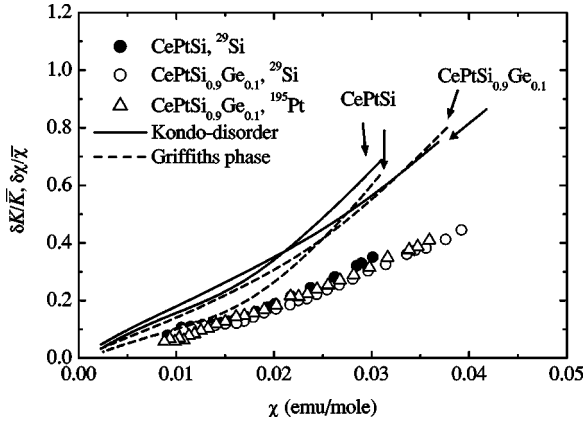

FIG. 11. A plot of the relative spread $\delta\chi/\overline{\chi}$ of susceptibility from disorder model fits over the entire temperature range and relative spread $\delta K/\overline{K}$ of frequency shift from NMR measurements plotted versus *ab*-plane bulk susceptibility χ for CePtSi and $CePtSi_{0.9}Ge_{0.1}$. Solid and dashed curves: predicted $\delta\chi/\overline{\chi}$ from Kondo-disorder and Griffiths phase models, respectively. Filled and open circles: $\delta K/\overline{K}$ from ^{29}Si NMR experiments in CePtSi and $CePtSi_{0.9}Ge_{0.1}$, respectively. Triangles: $\delta K/\overline{K}$ from ^{195}Pt NMR experiments in $CePtSi_{0.9}Ge_{0.1}$.

gests the existence of magnetic disorder in both materials.[10] Values of the relative width $\delta K/\overline{K}$ obtained from the NMR spectra are plotted against χ in Fig. 11. The data have been corrected for a small effect of disorder in the hyperfine coupling constant.[25] The $\delta K/\overline{K}$ curves for both samples show a strong dependence on the susceptibility (or temperature as an implicit parameter). They both increase at low temperatures (large χ) and are roughly linear in the susceptibility, as suggested by the disorder-driven NFL models.[10] In Fig. 11 it can be seen that the $\delta K/\overline{K}$ curves for the ^{29}Si NMR in CePtSi (filled circles) and $CePtSi_{0.9}Ge_{0.1}$ (open circles) almost overlap. This means that both samples have similar amounts of disorder in the local susceptibility, in agreement with our analysis of the bulk susceptibility (Sec. II D).

^{195}Pt NMR spectra were also obtained in $CePtSi_{0.9}Ge_{0.1}$ for comparison with the ^{29}Si spectra in the same material. We find that both spectra have similar Lorentzian-type line shapes, but ^{195}Pt spectra have larger shifts and are much broader than ^{29}Si spectra ($\sim 4\times$ wider at 4.2 K). ^{195}Pt usually shows a strongly shifted and broadened spectrum because of the strong atomic hyperfine interaction. Even with this stronger interaction, the $\delta K/\overline{K}$ data for ^{195}Pt NMR (triangles in Fig. 11) in $CePtSi_{0.9}Ge_{0.1}$ is still found to coincide with the data for ^{29}Si NMR (circles). This suggests that determination of the magnetic disorder from NMR spectra is independent of the probe nucleus, as expected because ^{195}Pt and ^{29}Si have the same number of Ce^{3+} near neighbors (Fig. 1), and the expression for $\delta K/\overline{K}$ [Eq. (9)] is the same for both nuclei.

The solid and dashed curves in Fig. 11 represent the relative spread of the susceptibility $\delta\chi/\overline{\chi}$ predicted by the Kondo-disorder and Griffiths phase models, respectively. Equations (2)–(5) and the second moment of the local susceptibility distribution

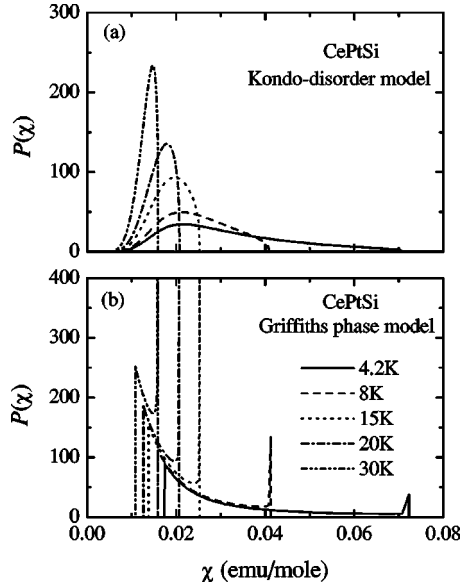

FIG. 12. Distributions $P(\chi)$ of the local susceptibilities estimated in CePtSi by (a) Kondo-disorder and (b) Griffiths phase models at various temperatures. The asymmetry and broadening in $P(\chi)$ are enhanced at low temperatures. The singularities at high-χ ends of $P(\chi)$ in (b) come from a Griffiths phase singularity ($\lambda < 1$) in Eq. (5) as the local energy $E \to 0$.

$$\overline{\chi^2} = \int_0^\infty \chi^2 P(\chi) d\chi \tag{10}$$

have been used to calculate $\delta\chi$ and $\delta\chi/\overline{\chi}$ using the fit parameters obtained from the disorder model fits for the entire temperature range as discussed in Sec. II D. The $\delta\chi/\overline{\chi}$ curves in Fig. 11 show that as found previously[25] the Kondo-disorder and the Griffiths phase models have similar predictions in both samples, and the difference in $\delta\chi/\overline{\chi}$ is not enough to discriminate between the Kondo-disorder and Griffiths phase models.

The expected relation between $\delta\chi/\overline{\chi}$ and $\delta K/\overline{K}$ is given by Eq. (9) with $A=0$. Clearly the $\delta K/K$ curves are lower than the $\delta\chi/\overline{\chi}$ curves in Fig. 11. Comparison with Eq. (9) suggests that the short-range correlation limit is applicable for both samples if a reasonable effective number n_{eff} of near-neighbor f ions can be obtained. A discussion of n_{eff} is given in the following section.

B. NMR line shape

The study of NMR line shapes has provided another way to examine the disorder-driven NFL models. Since the ^{29}Si and ^{195}Pt NMR spectra possess simple intrinsic line shapes without any quadrupolar satellites, detailed comparison of the measured spectra with the disorder-driven model calculated spectra becomes possible.

In disorder-driven models, the distribution function for the local susceptibility can be derived from Eqs. (2), (4), and (5). Figure 12 shows the distribution functions $P(\chi)$ for the susceptibilities in CePtSi at various temperatures predicted by the Kondo-disorder and Griffiths phase models, respec-

tively. Significant asymmetry in the distribution functions is seen in both models, and the spread as well as the asymmetry is enhanced at low temperatures. The singularities on the high-χ ends of $P(\chi)$ shown in Fig. 12(b) are due to the Griffiths singularity ($\lambda<1$) in the distribution function as the local energy $E\rightarrow 0$ in Eq. (5). The cutoffs on the low-χ ends are due to the upper energy cutoff in Eq. (5). If the NMR line broadening is interpretable by the disorder models, it might be expected that the NMR spectra should also exhibit asymmetry, because of the linear relation between the frequency shift and the local susceptibility [Eq. (6)]. We therefore need to understand why the observed NMR lines (Fig. 9) are essentially symmetric. In addition, we want to know if the line shape can discriminate between the Kondo-disorder and Griffiths phase models.

The calculation of the NMR spectrum is equivalent to finding the distribution function for the Knight shift $P(K)$. This can be obtained from the integral[50]

$$P(K)=\int \cdots \int P_n(k_1,k_2,\ldots,k_n)\delta\left(K-\sum_i^n k_i\right)dk_1dk_2\cdots dk_n, \tag{11}$$

where $P_n(k_1,k_2,\ldots,k_n)$ is the joint distribution function for the individual Knight shifts $k_i=a_i\chi_i$ [Eq. (6)] due to the surrounding magnetic ions. The integral is constrained by the delta function.

The strength of the hyperfine coupling between the NMR probe nucleus and the surrounding local moments is strongly dependent on the distance, but it decays rapidly because of $\sim 1/r^3$ dependence. Therefore, to simplify the calculation, we again introduce an effective number $n_{\rm eff}$ of near neighbors and an effective coupling constant $a_{\rm eff}$ ($k_i\approx a_{\rm eff}\chi_i$) as described in Sec. III A.

Assuming the variation of the local susceptibilities χ_i is not correlated (i.e., in the SRC limit), we can write $P_n(k_1,k_2,\ldots,k_n)=[P_0(k)]^{n_{\rm eff}}$, where $P_0(k)$ is the distribution function for each individual Knight shift (assumed the same for all magnetic ions). By expressing the delta function in the integral form $\delta(K-\Sigma_j\, k_j)=\int_{-\infty}^{\infty}\exp[i\tau(K-\Sigma_j\, k_j)]d\tau/(2\pi)$, the distribution function can be simplified to

$$P(K)=\int_{-\infty}^{\infty}e^{2\pi iK\tau}d\tau\left(\int_{-\infty}^{\infty}P_0(k)e^{-2\pi i\tau k}dk\right)^{n_{\rm eff}}. \tag{12}$$

For $k=a_{\rm eff}\chi$ the above equation becomes

$$P(K)=\frac{1}{a_{\rm eff}}\int_{-\infty}^{\infty}e^{2\pi i(K/a_{\rm eff})t}dt\left(\int_{-\infty}^{\infty}P(\chi)e^{-2\pi it\chi}d\chi\right)^{n_{\rm eff}}. \tag{13}$$

Clearly, the NMR spectrum is determined by $P(\chi)$ and the effective number of near neighbor Ce^{3+} ions around the probe nucleus. Therefore the NMR spectrum $P(K)$ can be calculated if $P(\chi)$ is known from the disorder models. If a_i is disordered, $P(K)$ still can be calculated by convoluting the above distribution function $P(K)$ with the distribution function $P(a)$ of the hyperfine coupling constant.

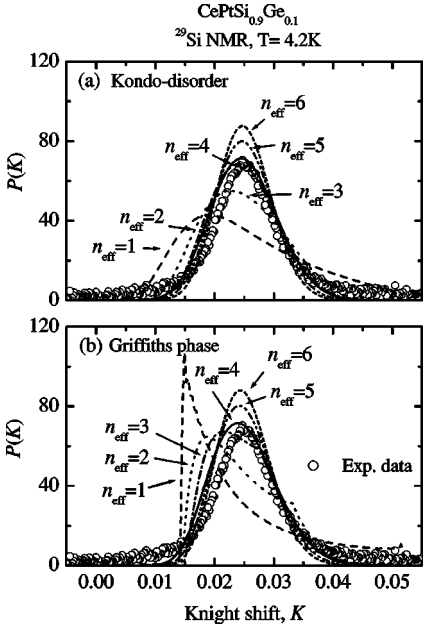

FIG. 13. Comparisons of normalized experimental ^{29}Si NMR spectra (circles) at 4.2 K in $CePtSi_{0.9}Ge_{0.1}$ with calculated spectra at various numbers $n_{\rm eff}$ of effective near neighbors. (a) Kondo-disorder model. (b) Griffiths phase model.

Comparisons of theoretical and experimental ^{29}Si NMR spectra at 4.2 K in $CePtSi_{0.9}Ge_{0.1}$ are given in Fig. 13. The small disorder in the hyperfine coupling constant discussed in the previous linewidth analysis has been included in the calculations. The theoretical spectra are plotted for various choices of the effective near-neighbor number $n_{\rm eff}$. For $n_{\rm eff}=1$, $P(K)=P(\chi)$ as given in Fig. 12. As $n_{\rm eff}$ increases, the asymmetry of $P(K)$ is reduced, and the line shape becomes more comparable to the observed spectrum. Calculated NMR spectra in both Kondo-disorder and Griffiths phase models are closest to the observed spectra when the effective number of near neighbors is around four, which is consistent with the linewidth analysis in Sec. III A. Although there is a small deviation, the calculated spectra reproduce the essential features of the observed spectra. However, the line shape study is still not able to distinguish between the Kondo-disorder and Griffiths phase models because of the smearing effect of coupling to $n_{\rm eff}$ near neighbors. According to the central limit theorem,[51] the line shape approaches a Gaussian if $n_{\rm eff}$ is large, independently of the distribution function for a single near neighbor. This effect can be seen in the calculated model spectra of Fig. 13. The line shape comparison for CePtSi is very similar to that for $CePtSi_{0.9}Ge_{0.1}$, and is omitted here.

From the theoretical spectra, the relative spreads of the Knight shifts $\delta K/\overline{K}$ at various $n_{\rm eff}$ are also obtained, and have been compared with the experimental data. Figure 14 give the comparison of $\delta K/\overline{K}$ in $CePtSi_{0.9}Ge_{0.1}$. The experimental data agree with the disorder models only when the effective number of the near neighbors is $n_{\rm eff}=3-4$ in $CePtSi_{0.9}Ge_{0.1}$. Similar treatment in CePtSi also gives $n_{\rm eff}=3-4$. Again these numbers are comparable with the crystal coordination numbers (Fig. 1).

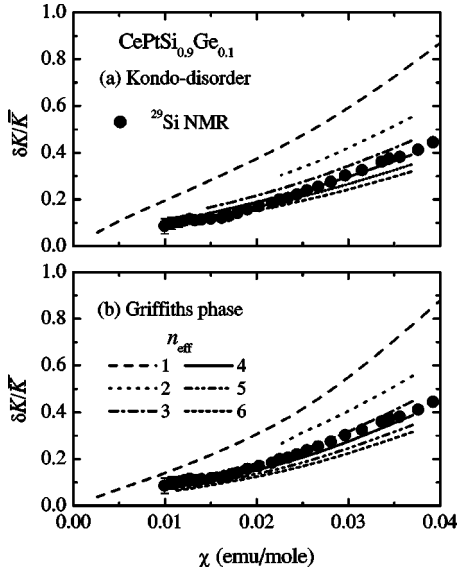

FIG. 14. Comparisons of $\delta K/\overline{K}$ obtained from (a) Kondo-disorder and (b) Griffiths phase models for various numbers n_{eff} of effective near neighbors in $CePtSi_{0.9}Ge_{0.1}$. Circles: experimental data.

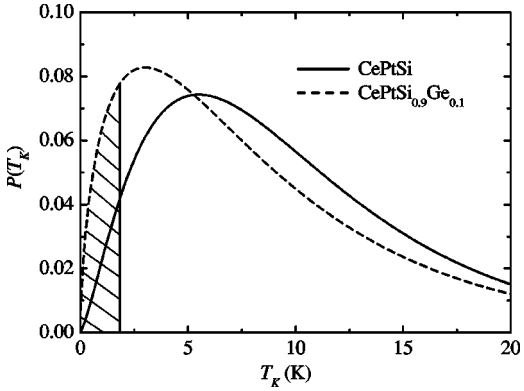

FIG. 15. Distributions of Kondo temperatures from Kondo-disorder model fits in CePtSi (solid curve) and $CePtSi_{0.9}Ge_{0.1}$ (dashed curve). The shaded area indicates the low-T_K spins which are not quenched at low temperatures and give rise to NFL behavior.

IV. DISORDER-DRIVEN NFL BEHAVIOR?

In Sec. III, we have seen that the Kondo-disorder and Griffiths phase models are able to describe the observed NMR line broadening and line shape. However, the similar magnitude of magnetic disorder seen in both CePtSi and $CePtSi_{0.9}Ge_{0.1}$ raises the question why only $CePtSi_{0.9}Ge_{0.1}$ shows NFL behavior. As we discussed in Sec. II B, the distribution of the Kondo temperatures is very sensitive to a small variation of the coupling constants g. Therefore the small differences in $\overline{g}$ and δg obtained from the fits of the susceptibility data for CePtSi and $CePtSi_{0.9}Ge_{0.1}$ (Sec. II D) may give an appreciable difference in the distribution of the Kondo temperatures, which can lead to different low temperature properties in the two materials.

In the Kondo-disorder picture, non-Fermi-liquid behavior appears only when there are enough unquenched local moments at low temperatures, i.e., when there is a substantial probability of finding local moments with low T_K. Figure 15 gives the distribution function of the Kondo temperatures in CePtSi and $CePtSi_{0.9}Ge_{0.1}$, obtained from Eq. (4) using the fit parameters from the Kondo-disorder model fits over the entire temperature range. It shows that although the T_K distributions for CePtSi and $CePtSi_{0.9}Ge_{0.1}$ have comparable widths, $CePtSi_{0.9}Ge_{0.1}$ has a smaller (average) Kondo temperature, so that the distribution function $P(T_K)$ is moved closer to the origin. This gives extra weight to the low-T_K spins in $CePtSi_{0.9}Ge_{0.1}$ compared with $P(T_K \to 0)=0$ in CePtSi (shaded area in Fig. 15), which then is able to explain the NFL behavior in $CePtSi_{0.9}Ge_{0.1}$ and FL behavior in CePtSi.

According to the Griffiths phase model, the critical exponent λ characterizes the ground state properties. From the susceptibility fits to the Griffiths phase model over the entire temperature range (Sec. II D), for CePtSi and $CePtSi_{0.9}Ge_{0.1}$ $\lambda = 1.51(4)$ and $\lambda = 1.01(1)$, respectively. Therefore the Griffiths phase model also can account for the FL behavior in CePtSi because of the lack of a Griffiths singularity for $\lambda > 1$. For $CePtSi_{0.9}Ge_{0.1}$ we find $\lambda \approx 1$, which suggests the system is close to a marginal Griffiths singularity at $\lambda = 1$ where log T behavior is expected.[12]

V. CONCLUSIONS

The linear extrapolation of the Wilson ratio to low temperatures in $CePtSi_{1-x}Ge_x$, $x=0$ and 0.1, enables us to estimate the magnetic susceptibility below 2 K, so that the distributions of local susceptibilities can be determined reasonably well by fits of the susceptibility to disorder-driven NFL models. NFL behavior in $CePtSi_{0.9}Ge_{0.1}$ and FL behavior in CePtSi are then found to be consistent with these fits as discussed in Sec. IV. Even though similar amounts of disorder are seen in CePtSi and $CePtSi_{0.9}Ge_{0.1}$, the slightly larger effect of disorder in $CePtSi_{0.9}Ge_{0.1}$ leads to $P(T_K \to 0) \neq 0$ (Kondo disorder) or $\lambda \approx 1$ (Griffiths phase) and NFL behavior in this compound.

The observed NMR linewidth and line shape in CePtSi and $CePtSi_{0.9}Ge_{0.1}$ are consistent with these fits to the disorder-driven NFL models. In the limit of short-range correlation between the local susceptibilities, the effective number of the near Ce^{3+} neighbors around the Si atom (3–4) is found to be close to the coordination number (4) for the first near-neighbor shell in the crystal structure. This agreement is confirmation that the disorder correlation is indeed short ranged. ^{195}Pt NMR experiments give an independent verification of the ^{29}Si NMR results. In addition, the disorder-driven NFL models are enough to explain the NFL behavior in $CePtSi_{0.9}Ge_{0.1}$, and no QCP scenario is needed to account for these data. We note, however, that μSR relaxation experiments in $UCu_{5-x}Pd_x$ (Ref. 52) cast doubt on a similar conclusion in this system[23] by suggesting that spin fluctuations are associated with a cooperative phase transition rather than individual spin dynamics.

Nevertheless, the comparable $\delta K/\overline{K}$ observed in CePtSi and $CePtSi_{0.9}Ge_{0.1}$ suggests that there is appreciable mag-

netic disorder in stoichiometric CePtSi. The relatively high residual resistivity $\rho_0 \approx 140\ \mu\Omega$ cm reported[53] in a single crystal of CePtSi supports this speculation. [Note that the effect of disorder on NFL behavior in $CeCu_{5.9}Au_{0.1}$, with lower residual resistivity ($\rho_0 \approx 40\ \mu\Omega$ cm),[54] is believed to be negligible.[23,28]] In addition, sample-dependent thermodynamic, magnetic, and transport properties in CePtSi have been reported,[55] and Köhler *et al.*[43] have suggested that possible disorder effects exist in this compound. If magnetic disorder is strong enough in undoped CePtSi, according to disorder-driven models it should be possible to see NFL behavior in a highly disordered sample. Introduction of disorder, e.g., by neutron irradiation, or a controlled annealing experiment as performed in UCu_4Pd (Ref. 27), would therefore be useful for further understanding of the FL/NFL behavior in CePtSi.

One of the common NFL properties, a linearly temperature-dependent resistivity ($\rho = \rho_0 + AT$), has been observed in CePtSi from 0.05 to 4 K and reported in Ref. 55. However, disorder-driven models cannot explain the positive slope ($A > 0$); according to the Kondo-disorder model, A should be negative.[11] From the table of NFL properties in different categories of materials published in Ref. 3, we find that $d\rho/dT < 0$ is seen in most materials with antiferromagnetism distant in the phase diagram, whereas $d\rho/dT > 0$ is seen in most doped materials with the Néel (or Curie) temperature suppressed to zero. The positive slope in CePtSi may also suggest a QCP scenario for the NFL behavior. As we know both CePtSi and $CePtSi_{0.9}Ge_{0.1}$ are located close to a magnetic instability. CePtSi is near a ferromagnetic phase transition,[56] and $CePtSi_{0.9}Ge_{0.1}$ is at an antiferromagnetic QCP. Therefore a QCP scenario for NFL behavior cannot be excluded in either case.

The NMR line shapes from our experiments do not distinguish between the Kondo-disorder and Griffiths phase models because they do not yield detailed information on the shape of the susceptibility distribution function. This is because each ^{29}Si nucleus couples to several near-neighbor Ce^{3+} ions. According to the central limit theorem,[51] in the limit of many near neighbors the field distribution approaches a Gaussian, so that details of the susceptibility distribution are lost.

In order to determine which if any of these models are valid, and to study further the role of structural disorder on NFL behavior in this system, nuclear spin-lattice relaxation measurements have been carried out and will be reported in a future publication.

ACKNOWLEDGMENTS

We gratefully thank Jungsoo Kim for measuring the susceptibility (2–300 K) of our CePtSi and $CePtSi_{0.9}Ge_{0.1}$ samples. Enlightening discussion with N. J. Curro is acknowledged. This research was supported by the U.S. NSF, Grant Nos. DMR-9731361 and DMR-0102293 (UC Riverside), DMR-0335173 (UC San Diego), and DMR-9820631 (CSU Los Angeles), and was carried out in part under the auspices of the U.S. DOE Contract No. DE-FG05-86ER45268. Research at Whittier College was supported by a grant from the Research Corporation, and by a ROA addendum to NSF Grant No. DMR-9731361.

*Present address: Condensed Matter and Thermal Physics, Los Alamos National Laboratory, Los Alamos, New Mexico 87545.

†Present address: Department of Physics, Kyoto University, Kyoto 606-8502, Japan.

[1] L. D. Landau, Sov. Phys. JETP **3**, 920 (1957).

[2] A. J. Schofield, Contemp. Phys. **40**, 95 (1999).

[3] G. R. Stewart, Rev. Mod. Phys. **73**, 797 (2001).

[4] C. M. Varma, Z. Nussinov, and W. van Saarloos, Phys. Rep. **361**, 267 (2002).

[5] D. L. Cox and M. Jarrell, J. Phys.: Condens. Matter **8**, 9825 (1996).

[6] D. L. Cox, Phys. Rev. Lett. **59**, 1240 (1987).

[7] A. J. Millis, Phys. Rev. B **48**, 7183 (1993).

[8] A. M. Tsvelik and M. Reizer, Phys. Rev. B **48**, 9887 (1993).

[9] T. Moriya and T. Takimoto, J. Phys. Soc. Jpn. **64**, 960 (1995).

[10] O. O. Bernal, D. E. MacLaughlin, H. G. Lukefahr, and B. Andraka, Phys. Rev. Lett. **75**, 2023 (1995).

[11] E. Miranda, V. Dobrosavljevic, and G. Kotliar, J. Phys.: Condens. Matter **8**, 9871 (1996).

[12] A. H. Castro Neto, G. Castilla, and B. A. Jones, Phys. Rev. Lett. **81**, 3531 (1998).

[13] A. H. Castro Neto and B. A. Jones, Phys. Rev. B **62**, 14 975 (2000).

[14] H. von Löhneysen, J. Phys.: Condens. Matter **8**, 9689 (1996).

[15] B. Bogenberger and H. von Löhneysen, Phys. Rev. Lett. **74**, 1016 (1995).

[16] K. Heuser, E.-W. Scheidt, T. Schreiner, and G. R. Stewart, Phys. Rev. B **57**, R4198 (1998).

[17] M. B. Maple, M. C. de Andrade, J. Herrmann, Y. Dalichaouch, D. A. Gajewski, C. L. Seaman, R. Chau, R. Movshovich, M. C. Aronson, and R. Osborn, J. Low Temp. Phys. **99**, 223 (1995).

[18] R. Chau and M. B. Maple, J. Phys.: Condens. Matter **8**, 9939 (1996).

[19] P. Gegenwart, F. Kromer, M. Lang, G. Sparn, C. Geibel, and F. Steglich, Phys. Rev. Lett. **82**, 1293 (1999).

[20] O. Trovarelli, C. Geibel, S. Mederle, C. Langhammer, F. M. Grosche, P. Gegenwart, M. Lang, G. Sparn, and F. Steglich, Phys. Rev. Lett. **85**, 626 (2000).

[21] F. Steglich *et al.*, Z. Phys. B: Condens. Matter **103**, 235 (1997).

[22] J. L. Gavilano, J. Hunziker, and H. R. Ott, Phys. Rev. B **52**, 13106 (1995).

[23] O. O. Bernal *et al.*, Phys. Rev. B **54**, 13000 (1996).

[24] M. C. de Andrade *et al.*, Phys. Rev. Lett. **81**, 5620 (1998).

[25] C.-Y. Liu, D. E. MacLaughlin, A. H. Castro Neto, H. G. Lukefahr, J. D. Thompson, J. L. Sarrao, and Z. Fisk, Phys. Rev. B **61**, 432 (2000).

[26] C. H. Booth, D. E. MacLaughlin, R. H. Heffner, R. Chau, M. B. Maple, and G. H. Kwei, Phys. Rev. Lett. **81**, 3960 (1998).

[27] A. Weber, S. Körner, E.-W. Scheidt, S. Kehrein, and G. R. Stewart, Phys. Rev. B **63**, 205116 (2001).
[28] H. von Löhneysen, J. Magn. Magn. Mater. **200**, 532 (1999).
[29] S. Horn, A. Mehner, C. Kämmerer, B. Seidel, C. D. Bredl, C. Geibel, and F. Steglich, J. Magn. Magn. Mater. **108**, 205 (1992).
[30] F. Steglich, C. Geibel, K. Gloos, G. Olesch, C. Schank, C. Wassilew, A. Loidl, A. Krimmel, and G. R. Stewart, J. Low Temp. Phys. **95**, 3 (1994).
[31] D. E. MacLaughlin, M. S. Rose, B.-L. Young, O. O. Bernal, R. H. Heffner, G. D. Morris, K. Ishida, G. J. Nieuwenhuys, and J. E. Sonier, Physica B **326**, 381 (2003).
[32] A. Krimmel, A. Severing, A. Murani, A. Grauel, and S. Horn, Physica B **180&181**, 191 (1992).
[33] T. Götzfried, A. Weber, K. Heuser, D. Maurer, E.-W. Scheidt, S. Kehrein, and G. R. Stewart, J. Low Temp. Phys. **127**, 51 (2002).
[34] R. B. Griffiths, Phys. Rev. Lett. **23**, 17 (1969).
[35] W. H. Lee and R. N. Shelton, Phys. Rev. B **35**, 5369 (1987).
[36] A. C. Hewson, *The Kondo Problem to Heavy Fermions* (Cambridge University Press, Cambridge, 1993).
[37] M. T. Hutchings, Solid State Phys. **16**, 227 (1964).
[38] I. Aviani, M. Miljak, V. Zlatic, K.-D. Schotte, C. Geibel, and F. Steglich, Phys. Rev. B **64**, 184438 (2001).
[39] L. Rebelsky, K. Reilly, S. Horn, H. Borges, J. D. Thomson, J. O. Willis, R. Aikin, R. Caspari, and C. D. Bredl, J. Appl. Phys. **63**, 3405 (1988).
[40] S. Maekawa, S. Kashiba, S. Takahashi, and M. Tachiki, J. Magn. Magn. Mater. **52**, 149 (1985).
[41] M. Lee, G. F. Moores, Y. Q. Song, W. P. Halperin, W. W. Kim, and G. R. Stewart, Phys. Rev. B **48**, 7392 (1993).
[42] B.-L. Young, M. S. Rose, D. E. MacLaughlin, K. Ishida, O. O. Bernal, H. G. Lukefahr, K. Heuser, E. J. Freeman, and M. B. Maple, Rev. Sci. Instrum. **73**, 3038 (2002).
[43] R. Köhler, B. Strobel, C. Kämmerer, A. Grauel, U. Gottwick, E. Göring, A. Höhr, G. Sparn, C. Geibel, and S. Horn, J. Magn. Magn. Mater. **90&91**, 428 (1990).
[44] K. G. Wilson, Rev. Mod. Phys. **47**, 773 (1975).
[45] The anomalously small uncertainties in the fit parameters arise from the fact that other parameters were fixed.
[46] R. Chau, M. B. Maple, and R. A. Robinson, Phys. Rev. B **58**, 139 (1998).
[47] G. C. Carter, L. H. Bennett, and D. J. Kahan, Prog. Mater. Sci. **20**, 1 (1977).
[48] W. G. Clark, M. E. Hanson, F. Lefloch, and P. Segransan, Rev. Sci. Instrum. **66**, 2453 (1995).
[49] D. E. MacLaughlin, O. O. Bernal, and H. G. Lukefahr, J. Phys.: Condens. Matter **8**, 9855 (1996).
[50] R. E. Walstedt and L. R. Walker, Phys. Rev. B **9**, 4857 (1974).
[51] F. Reif, *Fundamentals of Statistical and Thermal Physics* (McGraw–Hill, Singapore, 1965).
[52] D. E. MacLaughlin, O. O. Bernal, R. H. Heffner, G. J. Nieuwenhuys, M. S. Rose, J. E. Sonier, B. Andraka, R. Chau, and M. B. Maple, Phys. Rev. Lett. **87**, 066402 (2001).
[53] M. Sera, T. Satoh, and T. Kasuya, J. Phys. Soc. Jpn. **57**, 671 (1988).
[54] H. von Löhneysen, J. Phys.: Condens. Matter **8**, 9689 (1996).
[55] H. R. Ott, E. Felder, S. Takagi, A. Schilling, N. Sato, and T. Komatsubara, Philos. Mag. B **65**, 1349 (1992).
[56] W. H. Lee, H. C. Ku, and R. N. Shelton, Phys. Rev. B **38**, 11 562 (1988).